

Effect of $\pi\pi$ interactions in πN scattering

John A. Johnstone and T.-S. H. Lee

Physics Division, Argonne National Laboratory, Argonne, Illinois 60439

(Received 26 February 1986)

The standard cloudy bag model description of πN scattering is extended to include contributions at the two-pion level. The $\pi\pi$ scattering amplitudes are parametrized in phenomenological, separable forms consistent with the known $\pi\pi$ S - and P -wave phase shifts. These amplitudes are embedded in the πN description to account for scattering of the incident pion from the nucleon's virtual pion cloud. A self-consistent analysis of the coupled πN , $\pi\Delta$, and πN^* (1470) systems results in excellent reproduction of the phase shifts in the πN P_{33} channel to energies above the pion production threshold. In the P_{11} channel, without two-pion intermediate states, no acceptable fit to the data is possible for any values of the bag parameters. It is shown that the additional attraction provided by $\pi\pi$ scattering is essential to reproduce the low-energy phase shifts and fix the sign change at the correct energy.

I. INTRODUCTION

The πN interactions form the foundation for the description of NN and πd reactions. To account for the absorption-production processes $NN \leftrightarrow \pi NN$ and $NN \leftrightarrow \pi d$ the underlying πN model must contain vertex interactions $\pi B \leftrightarrow B'$, where in general B and B' can be N , Δ , or higher mass nucleon resonances. An accurate description of the P_{33} πN channel can be obtained easily¹ with a $\pi N \leftrightarrow \Delta$ vertex interaction, but a tractable P_{11} model with vertex interactions is much more difficult to construct. The P_{11} channel phase shifts^{2,3} are very small ($|\delta| < 1.5^\circ$), but negative, from threshold to pion kinetic energies of $T_\pi \sim 170$ MeV, then rise gradually through the resonance at $T_\pi \sim 530$ MeV. Roughly the low energy repulsion results from the nucleon pole and the high energy attraction from excitation of the $N^*(1470)$, but the precise behavior of the low energy phase shifts requires nearly perfect cancellation between attractive and repulsive mechanisms. Clearly, the P_{11} channel is sensitive to the details of πN dynamics.

Probably the simplest P_{11} model comprises a nucleon pole term and a phenomenological background interaction parametrized as a low-rank separable interaction. The parameters of the model are fixed by fitting both the P_{11} phases and the position of the nucleon pole. This procedure was proposed by Mitzutani and Koltun⁴ and used in most subsequent πNN calculations. However, this simple approach is not satisfactory since it can be seen from several existing calculations⁵ that the calculated NN and πd polarization cross sections, in particular, are sensitive to the parametrization of the background term.

Additional dynamical input is therefore required to reduce the uncertainties in constructing a P_{11} model. One possibility is to insist that the model reproduce the πN phase shifts to a higher energy region where $\pi N \rightarrow \pi\pi N$ production processes can occur. This idea has been applied by Blankleider and Walker,⁶ and also by McLeod and Afnan.⁷ Both of these approaches essentially extended the separable model to account for πN inelasticity but

without introducing explicit vertex mechanisms for N^* excitation and its associated pion production. It still remains to be seen whether πNN calculations become insensitive to the parametrization when higher energy πN data are included to constrain the model.

Experimentally, the N^* is known to have a large decay width⁸ for the transition $N^* \rightarrow \pi\Delta \rightarrow \pi\pi N$. This 2π mechanism is included in the isobar model for N^* excitation constructed by Lee⁹ in his study of NN scattering up to 2 GeV. This model was later extended by Bhalerao and Liu¹⁰ to include η production, but neither model deals with the important nucleon pole term and hence are adequate only at energies high enough to be dominated by N^* excitation.

A more fundamental approach is to relate the $\pi B \leftrightarrow B'$ vertex interactions to the underlying quark-pion dynamics. This has been attempted via the cloudy bag model¹¹ (CBM) in particular. In this approach the number of model parameters is greatly constrained by fixing the relative coupling strengths at vertices through the quark structure of the baryons. While it has been demonstrated¹² that the CBM is consistent with the πN P_{33} phase shifts below π production threshold, it has been less successful in predictions about the P_{11} channel. Rinat¹³ tried to fit the P_{11} scattering data considering only N and N^* pole mechanisms, assuming the $N^*(1470)$ to be a $(0s)^2(1s)^1$ quark configuration. The resultant interaction was much too repulsive, producing phase shifts that dropped as low as $-20^\circ \rightarrow -30^\circ$. Brown *et al.*¹⁴ assumed the N^* resonance to be a breathing mode excitation of the nucleon and they predicted even greater repulsion at low energies. The difficulties encountered in these P_{11} analyses could be due, in part at least, to an incomplete description of the N^* excitation.

While the N and N^* pole terms [Fig. 1(a)] are undoubtedly the dominant mechanisms in the P_{11} channel, to the order of the πN coupling constant squared, processes like Figs. 1(b) and (c) must also contribute. The crossed graphs are suppressed through spin-isospin considerations and large energy denominators, but nonetheless, in the P_{11}

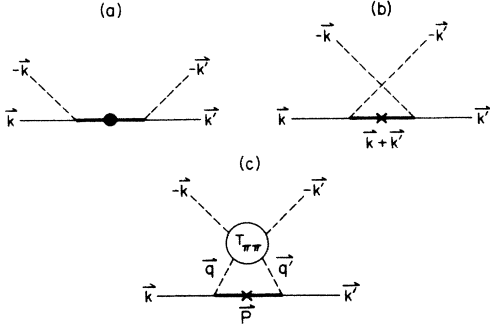


FIG. 1. Generic contributions to πN scattering. Dashed lines are pions and solid lines are nucleons. In general, the intermediate state baryons (solid bars) may be any of N , Δ , or N^* . In (c) the circle represents the $\pi\pi$ interactions.

channel crossed terms with N , Δ , and N^* intermediate states can all contribute. These are attractive and tend to counteract the N -pole repulsion. Interactions of the type in Fig. 1(c), in which the incident pion scatters from the virtual pion cloud, have not been considered previously but they are expected to be significant because of the $S^*(980)$ and $\rho(760)$ resonances in the $I=J=0$ and $I=J=1$ $\pi\pi$ channels. Their inclusion could provide another source of low energy attraction in P_{11} to counteract the N -pole repulsion.

Our primary interest in this paper is to examine the role of the $\pi\pi$ interactions in πN scattering. To accomplish this we consider a πN model in which the πN scattering equation incorporates the three classes of driving terms depicted in Fig. 1, and simultaneously makes contact with the concepts of quark-pion physics. In the following section we present the model for the $\pi B \leftrightarrow B'$ vertex interactions and the explicit forms of the driving terms of Figs. 1(a) and (b) derived from these interactions. The $\pi\pi$ scattering amplitudes are constructed phenomenologically in Sec. III from the experimental $\pi\pi$ phase shifts. The πN scattering problem is then solved in the approximation that only intermediate states up to the 2π level are included to account for πN inelasticities. The results of the simultaneous fit to the πN P_{11} and P_{33} channels are presented and discussed in Sec. IV.

II. $\pi B \leftrightarrow B'$ VERTEX INTERACTIONS AND πN SCATTERING

We start with the πN scattering equation deduced in a perturbative expansion of the exact CBM πN scattering amplitude discussed in Ref. 11. The resulting scattering equation is of the following familiar Lippmann-Schwinger form:

$$t_{\pi N}(E) = v(E) + v(E) \frac{1}{E - H_0 + i\epsilon} t_{\pi N}(E), \quad (2.1)$$

where $v(E)$ is the sum of the first two driving terms illustrated in Fig. 1 and H_0 is the sum of the free (relativistic) pion and nucleon energies. To study the effect due to pion scattering from the pion cloud of the nucleon we

simply add a $\pi\pi$ scattering driving term [Fig. 1(c)], called $V_{\pi\pi}$, to $v(E)$.

Obviously, if we hope to distinguish the second-order $\pi\pi$ correlation effects, the number of model parameters must be severely restricted. We therefore take guidance from the CBM and interrelate all vertex strengths via $SU(6)$. The general $\pi BB'$ vertex functions are then assumed to be of the form

$$h(\mathbf{k}) = (2\pi)^{-3/2} \frac{f^0 u(kR)}{m_\pi (2\omega_k)^{1/2}} (\hat{\mathbf{S}} \cdot \mathbf{k})(\hat{\mathbf{T}} \cdot \boldsymbol{\phi}) \quad (2.2)$$

with m_π and ω_k the pion's mass and energy, respectively, $\boldsymbol{\phi}$ is the pion isovector field, and $u(kR)$ is a cutoff function which is taken to be parametrized in the CBM form

$$u(kR) = 3j_1(kR)/kR \quad (2.3)$$

with $j_l(x)$ being the $l=1$ spherical Bessel function, and R the bag radius, assumed to be the same for all baryons. The coupling constant f^0 in Eq. (2.2) is the bare $NN\pi$ coupling constant [the experimental value of $f_{NN\pi}$ is ~ 1 with the choice of normalization in Eq. (2.2)]. All other $BB'\pi$ coupling strengths are related to $f_{NN\pi}$ by $SU(6)$ symmetry. In units of $f_{NN\pi}$ we have

$$\begin{aligned} f_{NN\pi} &= 1, \\ f_{\Delta N\pi} &= 6\sqrt{2}/5, \end{aligned} \quad (2.4)$$

and

$$f_{\Delta\Delta\pi} = \frac{4}{5}.$$

The spin and isospin transition operators, $\hat{\mathbf{S}}$ and $\hat{\mathbf{T}}$, are defined via their reduced matrix elements as

$$\begin{aligned} \langle sv | S_x | s'v' \rangle &= (-)^{s'+v'+1+x} \\ &\times \begin{pmatrix} s' & 1 & s \\ v' & x & -v \end{pmatrix} \langle s || \hat{\mathbf{S}} || s' \rangle, \end{aligned} \quad (2.5a)$$

with

$$\begin{aligned} \langle \frac{1}{2} || \hat{\mathbf{S}} || \frac{1}{2} \rangle &= \sqrt{6}, \\ \langle \frac{1}{2} || \hat{\mathbf{S}} || \frac{3}{2} \rangle &= \langle \frac{3}{2} || \hat{\mathbf{S}} || \frac{1}{2} \rangle = 2, \end{aligned} \quad (2.5b)$$

and

$$\langle \frac{3}{2} || \hat{\mathbf{S}} || \frac{3}{2} \rangle = \sqrt{15}.$$

The reduced matrix elements of $\hat{\mathbf{T}}$ are identical to those of Eq. (2.5b).

Assuming the bare N^* to have a $(0s)^2(1s)^1$ quark structure, and using the explicit quark wave functions,¹¹ the $N^* \leftrightarrow B\pi$ coupling constants can also be determined. For example

$$f_{N^*N\pi} = \left[\frac{\omega_1(\omega_0 - 1)}{3\omega_0(\omega_1 - 1)} \right]^{1/2} f_{NN\pi} = 0.4570 f_{NN\pi}, \quad (2.6)$$

where $\omega_0 = 2.043$ and $\omega_1 = 5.395$ are the eigenfrequencies of the $0s$ and $1s$ quarks. Similarly, the other relevant N^* couplings are $f_{N^*\Delta\pi} = 0.4570 f_{\Delta N\pi}$, and $f_{N^*N^*\pi} = 0.8755 f_{NN\pi}$.

The driving terms of Figs. 1(a) and (b) projected onto the πN channel of isospin I , total angular momentum J , and incident energy E are

$$\sum_B \alpha_{NB} \frac{f_{NB}(k)kk'f_{BN}(k')}{E - M_B^0 - \Sigma_B(E)}, \quad (2.7)$$

$$\sum_B \frac{\beta_{NB} f_{NB}(k')k'kf_{BN}(k)}{E - \omega_k - \omega_{k'} - E_B^0[(k^2 + k'^2)^{1/2}] - \sigma_B[E - \omega_k - \omega_{k'}; (k^2 + k'^2)^{1/2}]}, \quad (2.8)$$

where $f_{NB}(k)$ is related to the CBM form factor by

$$f_{NB}(k) = (2\pi)^{-3/2} \frac{f_{NB\pi} u(kR)}{m_\pi (2\omega_k)^{1/2}}. \quad (2.9)$$

The coefficients α and β giving the relative strengths of the terms are constructed from the spin, isospin matrix elements of the vertex functions. In the pole terms [Eq. (2.7)] these have the value

$$\alpha_{NB} = \frac{4\pi}{3} \frac{\langle S_N || \hat{S} || S_B \rangle^2 \langle I_N || \hat{T} || I_B \rangle^2}{(2J+1)(2T+1)} \delta_{J,A_B} \delta_{T,I_B} \quad (2.10)$$

and in the crossed diagrams [Eq. (2.8)]

$$\beta_{NB} = \frac{4\pi}{3} \begin{Bmatrix} 1 & S_N & J \\ 1 & S_N & S_B \end{Bmatrix} \begin{Bmatrix} 1 & I_N & T \\ 1 & I_N & I_B \end{Bmatrix} \times \langle S_N || \hat{S} || S_B \rangle^2 \langle I_N || \hat{T} || I_B \rangle^2. \quad (2.11)$$

In the above equations $S_B = I_B = \frac{1}{2}, \frac{3}{2}, \frac{1}{2}$ for $B = N, \Delta,$ and N^* , respectively. In the propagators of Eqs. (2.7) and (2.8) M_B^0 and E_B^0 are the mass and energy of the bare baryon, with B being any of $N, \Delta,$ and N^* consistent with spin and isospin conservation. Following Ref. 9, the self-energies of the isobars to the level of 2π virtual states are taken to be

$$\Sigma_B(E) = \sum_R \alpha_{BR} \int \frac{dk k^4 f_{BR}^2(k)}{E^+ - \omega_k - E_R^0(k) - \sigma_R(E - \omega_k; k)}, \quad (2.12)$$

$$\sigma_R(E - \omega_k; k)$$

$$= \sum_S \alpha_{RS} \int \frac{dp p^4 f_{RS}^2(p)}{E^+ - \omega_k - \{[\omega_p + E_S^0(p)]^2 + k^2\}^{1/2}}. \quad (2.13)$$

The sums in both equations extend over the combinations of $R, S = N, \Delta,$ and N^* allowed by spin and isospin conservation. It is the second term above, Eq. (2.13), that describes the coupling to the $\pi\pi N$ inelastic channel in our model and hence is the source of πN inelasticity above the pion production threshold. The self-energy contributions defined by Eqs. (2.12) and (2.13) are depicted graphically in Fig. 2(a).

Strictly, the self-energy corrections due to crossed processes, such as those illustrated in Fig. 2(b), should also be included. These are suppressed through spin and isospin constraints and large energy denominators and are found to contribute about 10% of the terms of Fig. 2(a). It has also been shown¹⁵ that these terms can be absorbed into the processes of Fig. 2(a) by using a renormalized vertex

function. This refinement is not significant for our purpose and is neglected here.

As they stand, the propagators of the driving terms are defined exclusively in terms of the bare particles. For the Δ and N^* the "physical" particles are unstable, so there is no obvious advantage to renormalizing the masses. The nucleon on the other hand is stable and it is desirable to express quantities in terms of the physical nucleon mass. The nucleon pole is identified in the usual way by demanding that at $E = M_N$ the denominator of the term with nucleon intermediate state in Eq. (2.17) vanish. That is

$$M_N \equiv M_N^0 + \Sigma_N(M_N). \quad (2.14)$$

Notice that $\Sigma_N(E)$, as defined in Eq. (2.12), is a function of the bare nucleon mass M_N^0 through σ_N [Eq. (2.13)]. Therefore Eq. (2.14) is a highly nonlinear equation relating M_N to the bare mass M_N^0 through the interaction Hamiltonian. To simplify the calculation we use an approximation based on the observation that the self-energies $\Sigma_N(E)$ and $\sigma_N(E)$ vary slowly as $E \rightarrow M_N$. We can therefore approximate

$$E - M_N^0 - \Sigma_N(E) \rightarrow (E - M_N) \left[1 - \frac{\partial \Sigma_N(E')}{\partial E'} \Big|_{E'=M_N} \right], \quad (2.15)$$

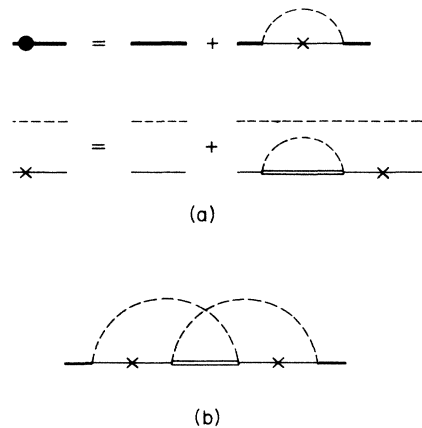


FIG. 2. Definition of the propagators and self-energy corrections used in Fig. 1, and in Eqs. (2.7) and (2.8). The solid circle and \times in (a) represent self-energy corrections to the 2π level, and 1π in the presence of a spectator pion, respectively; (b) shows an example of a 2π self-energy term which can be absorbed into those of (a) by renormalizing the vertex function.

which is exact at the pole. The right-hand side of Eq. (2.15) still depends on M_N^0 through the second-order self-energy correction $\sigma_N(E)$, so we extend the approximation to write the energy dependence of Eq. (2.12) as

$$E - \omega_k - E_N^0(k) - \sigma_N(E - \omega_k; k) \rightarrow [E - \omega_k - E_N(k)] \left[1 - \frac{\partial \sigma_N(\omega; k_0)}{\partial \omega} \Big|_{\omega=E_N(k_0)} \right] \quad (2.16)$$

with k_0 the πN on-shell momentum. This ensures that the π -“dressed N_0 ” has the correct physical πN elastic cut. Equations (2.15) and (2.16) allow us to carry out calculations without defining explicitly the bare nucleon mass M_N^0 .

In the crossed terms of Eq. (2.8) notice that we go beyond the 2π approximation by including the baryon self-energy defined by Eq. (2.13) in the $\pi\pi B$ propagator. This procedure essentially includes some, but not all, 3π terms in our calculation. These higher order terms are found to give additional attraction which improves the fit to the low energy P_{11} phase shifts.

To evaluate Eq. (2.8) we use an approximation similar to Eq. (2.16) to eliminate the bare nucleon mass. The final form for the nucleon propagator then becomes

$$\{E - \omega_k - \omega_{k'} - E_N[(k^2 + k'^2)^{1/2}]\} \times \left\{ 1 - \frac{\partial \sigma_N[\omega; (k^2 + k'^2)^{1/2}]}{\partial \omega} \Big|_{\omega=E_N[(k^2 + k'^2)^{1/2}]} \right\}. \quad (2.17)$$

Equations (2.7)–(2.17) completely define the driving terms of Figs. 1(a) and (b). Although the contributions to πN scattering from the vertex interactions of our model are more sophisticated than in earlier CBM studies due to the inclusion of the 2π channels, it is not anticipated that these will significantly alter the predictions of the *low* energy phase shifts from earlier studies.

III. $\pi\pi$ SCATTERING DRIVING TERM

To simplify the calculation of the terms of Fig. 1(c), we parametrize the $\pi\pi$ amplitude in each isospin, angular momentum channel I, l in separable form as

$$T_{\pi\pi}(\boldsymbol{\kappa}, \boldsymbol{\kappa}', E) = \sum_{IM} \langle 1\pi 1\pi' | I l \rangle^2 Y_{IM}^*(\hat{\boldsymbol{\kappa}}) \times T_l^I(\boldsymbol{\kappa}, \boldsymbol{\kappa}', E) Y_{IM}(\hat{\boldsymbol{\kappa}}') \quad (3.1a)$$

with

$$V_{\pi\pi}(\mathbf{k}, \mathbf{k}', E) = \sum_R \int \frac{d\mathbf{p} h_{NR}^*(\mathbf{q}) T_{\pi\pi}[\boldsymbol{\kappa}, \boldsymbol{\kappa}', E - E_R(p)] h_{RN}(\mathbf{q}')}{[\omega_q + E_R(k_0) - E_N(k_0)][\omega_{q'} + E_R(k_0) - E_N(k_0)]} \quad (3.3)$$

with $\mathbf{q} = \mathbf{k} - \mathbf{p}$, $\mathbf{q}' = \mathbf{k}' - \mathbf{p}$, and k_0 is the πN on-shell momentum. $T_{\pi\pi}$ is the fully off-shell $\pi\pi$ t matrix defined in Eq. (3.1) and the $h_{NR}(\mathbf{q})$ are the CBM vertex functions of Eq. (2.2). The intermediate state baryon R is N, Δ , or N^* . $V(\mathbf{k}, \mathbf{k}')$ is projected onto the πN channel of isospin I , orbital and total angular momentum L and J in the following

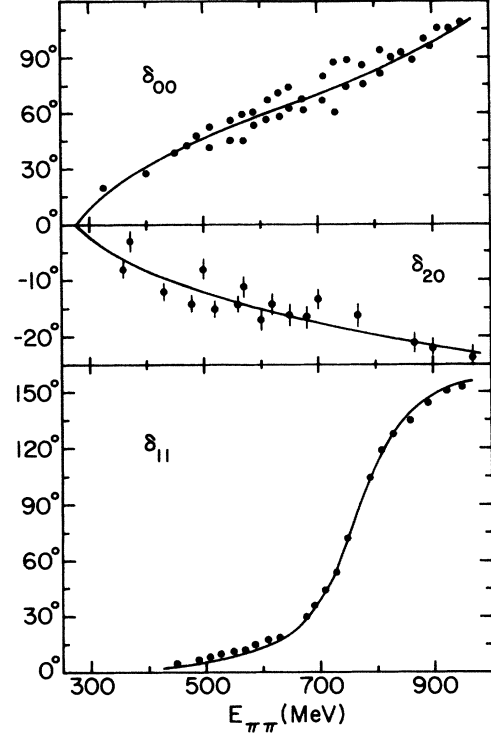


FIG. 3. Results of the fit to the $\pi\pi$ phase shifts (δ_{IJ}) in the lower partial waves. The data are taken from Ref. 16.

$$T_l^I(\boldsymbol{\kappa}, \boldsymbol{\kappa}', E) = v_{II}(\boldsymbol{\kappa}) D_l^I(E) v_{II}(\boldsymbol{\kappa}') \quad (3.1b)$$

and

$$D_l^I(E) = \left[E - M_{II}^0 - \int \frac{dp p^2 v_{II}^2(p)}{E + 2\omega(p)} \right]^{-1} \quad (3.1c)$$

and where $\boldsymbol{\kappa}, \boldsymbol{\kappa}'$ are the initial, final state $\pi\pi$ relative momenta, and the form factors $v_{II}(\boldsymbol{\kappa})$ are parametrized as

$$v_{II}(\boldsymbol{\kappa}) = g \frac{(\boldsymbol{\kappa}r)^l}{[1 + (\boldsymbol{\kappa}r)^2]^{l+1}}. \quad (3.2)$$

It is trivial to fit the $\pi\pi$ phase shifts with the above resonance-form parametrization of the t matrix. The best fits to the phase shifts δ_{IJ} (Ref. 16) in the three lowest $\pi\pi$ partial waves are shown in Fig. 3, and the best fit parameters are listed in Table I. The small, repulsive isospin = 2, S -wave channel was included for the sake of completeness, and it will turn out to be significant in the description of the P_{33} πN channel, as will be discussed later.

The potential due to the processes of Fig. 1(c) is then constructed to be

way. For a given $\pi\pi$ channel of isospin t and angular momentum l , $V_{\pi\pi}(\mathbf{k}, \mathbf{k}')$ is decomposed by using the following properties:

$$\frac{f_{NR}(q)v_R(\kappa)}{\omega_q + E_R(k_0) - E_N(k_0)} = \sum_{L'M'} C_{L'}^t(k;p) Y_{L'M'}^*(\hat{\mathbf{k}}) Y_{L'M'}(\hat{\mathbf{p}}) \quad (3.4a)$$

and

$$\langle S_N v | \hat{\mathbf{S}} \cdot \mathbf{q} | R r \rangle = \left[\frac{4\pi}{3} \right]^{1/2} \langle S_N || \hat{\mathbf{S}} || R \rangle (-1)^{R+1+v} \begin{pmatrix} S_N & 1 & R \\ -v & -\lambda_{-r} & r \end{pmatrix} q Y_{1,v-r}(\hat{\mathbf{q}}) \quad (3.4b)$$

with

$$q Y_{1,v-r}(\hat{\mathbf{q}}) = \sum_{Aab} \left[\frac{4\pi}{3} \right]^{1/2} k^{1-A} p^A (-1)^{1-A-v+R} \begin{pmatrix} A & 1-A & 1 \\ a & b & v-r \end{pmatrix} Y_{1-A,b}(\hat{\mathbf{k}}) Y_{Aa}(\hat{\mathbf{p}}). \quad (3.4c)$$

With some effort, the projection of $V_{\pi\pi}$ for intermediate state baryon R can be carried out to give

$$V_{LJ}^{\pi\pi}(k, k', E) = \sum_t U_{LJ}^t(k, k', E) \quad (3.5a)$$

with

$$U_{LJ}^t(k, k', E) = \int dp p^2 \lambda_{LJL'L''}^t(k, p, k') c_{L'}^t(k;p) c_{L''}^t(p;k') D_t^J[\omega - E_R(p)] \quad (3.5b)$$

with the momentum dependent coefficients $\lambda_{LJL'L''}^t(k, p, k')$ given by

$$\begin{aligned} \lambda_{LJL'L''}^t(k, p, k') &= (2I+1) \begin{Bmatrix} R & t & I \\ 1 & \frac{1}{2} & 1 \end{Bmatrix}^2 \langle 1/2 || \hat{\mathbf{T}} || R \rangle^2 \\ &\times \frac{3}{4\pi} \sum_{ABCEF} \hat{L}^2 \hat{t}^2 \hat{L}'^2 \hat{A}^2 \hat{B}^2 \hat{F}^2 \langle 1/2 || S || R \rangle^2 k^{1-C} (-p)^{C+E} k'^{1-E} (-)^{J+S+l+L+L'} \\ &\times \begin{pmatrix} L & l & A \\ 0 & 0 & 0 \end{pmatrix} \begin{pmatrix} A & 1-C & L' \\ 0 & 0 & 0 \end{pmatrix} \begin{pmatrix} L' & E & F \\ 0 & 0 & 0 \end{pmatrix} \begin{pmatrix} F & L'' & C \\ 0 & 0 & 0 \end{pmatrix} \begin{pmatrix} L' & l & B \\ 0 & 0 & 0 \end{pmatrix} \begin{pmatrix} B & 1-E & L'' \\ 0 & 0 & 0 \end{pmatrix} \\ &\times \sum_X \hat{X}^2 \begin{Bmatrix} 1 & A & X \\ L' & C & 1-C \end{Bmatrix} \begin{Bmatrix} L' & C & X \\ L'' & E & F \end{Bmatrix} \begin{Bmatrix} L'' & E & X \\ 1 & B & 1-E \end{Bmatrix} \begin{Bmatrix} 1 & \frac{1}{2} & L' & L \\ B & \frac{1}{2} & A & \frac{1}{2} \\ X & l & R & J \end{Bmatrix}. \quad (3.6) \end{aligned}$$

Specifically, in the P_{11} πN channel the λ become

$$R = N, l = 0, t = 0: c_0 d_0 k k' - c_1 d_0 k' p - c_0 d_1 k p + c_1 d_1 p^2, \quad (3.7a)$$

$$R = N, l = 1, t = 1: 2 \left[c_0 d_0 p^2 - c_1 d_0 \frac{kp}{3} + c_1 d_1 k k' \right], \quad (3.7b)$$

$$R = \Delta, l = 1, t = 1: \frac{16}{25} (c_0 d_0 p^2 - \frac{2}{3} c_1 d_0 k p - \frac{2}{3} c_0 d_1 k' p), \quad (3.7c)$$

and in the P_{33} channel:

$$R = N, l = 1, t = 1: \frac{36}{25} (c_0 d_0 p^2 - \frac{4}{9} c_1 d_0 k p - \frac{4}{9} c_0 d_1 k' p), \quad (3.8a)$$

$$R = \Delta, l = 0, t = 0: \frac{8}{25} (c_0 d_0 k k' - c_1 d_0 k' p - c_0 d_1 k p + c_1 d_1 p^2), \quad (3.8b)$$

$$R = \Delta, l = 0, t = 2: \frac{4}{5} (c_0 d_0 k k' - c_1 d_0 k' p - c_0 d_1 k p + c_1 d_1 p^2), \quad (3.8c)$$

$$R = \Delta, l = 1, t = 1: \frac{4}{5} \left[2c_0 d_0 p^2 - c_1 d_0 \frac{kp}{3} - c_0 d_1 \frac{k'p}{3} + c_1 d_1 k k' \right]. \quad (3.8d)$$

TABLE I. Parameters of the best fit to the $\pi\pi$ phase shifts with the separable potential model described in the text.

Channel (I, J)	$\frac{g}{m_\pi^{1/2}}$	r (fm)	M_{IJ}^0 (MeV)
(0,0)	0.7550	0.522	896.8
(1,1)	0.6684	0.428	811.7
(2,0)	0.6318	0.231	228.9

All of the above amplitudes are measured in units of $f_{\pi N \pi}^2$. The abbreviations have been used that $c_{L'} \equiv c_{L'}^t(k, p)$ and $d_{L''} \equiv d_{L''}^t(p, k')$. These two functions are calculated numerically according to Eq. (3.4a). In

each of P_{33} and P_{11} there are also the terms with an N^* in the intermediate state. These are identical with the ones given above for $R=N$, but there is an overall factor of $(0.4570)^2$. Also the N^* mass is much greater than that of N so these N^* terms do not contribute significantly, and can safely be neglected. Notice that the $l=0, t=2$ $\pi\pi$ channel contributes to P_{33} but not P_{11} . The significance of this term is that it is repulsive, and so tends to cancel against the other attractive $\pi\pi$ interactions. Because the $\pi\pi$ t matrix has been constructed consistently with the $\pi\pi$ phase shifts the inclusion of the correlated $\pi\pi$ terms in describing πN scattering does not introduce any additional parameters beyond those already contained in the $NR\pi$ vertex functions.

IV. RESULTS AND DISCUSSIONS

The πN scattering defined in Sec. III can be calculated as follows. For each πN partial wave one solves Eq. (2.1) with the driving term taken to be the sum of Eqs. (2.7), (2.8), and (3.5). The model has four free parameters; the $NN\pi$ coupling constant $f_{NN\pi}$, the bag radius R , and the bare masses of the Δ and N^* . Our task is therefore to determine these parameters by carrying out a χ^2 fit to the πN phase shifts up to about 2 GeV (total πN c.m. energy). At the 2π level the same parameters enter the P_{11} and P_{33} channel descriptions. For the model to be sensible it must therefore reproduce both partial waves simultaneously. In addition, the resulting bag parameters should not be very different from those determined in the original cloudy-bag model study, since in our approximation the 2π effect is considered to be a perturbative correction in describing the static properties of baryons.

To illustrate the necessity of including a $\pi\pi$ scattering mechanism, we first carry out a χ^2 fit neglecting the $\pi\pi$ scattering term $V_{\pi\pi}$ in the calculation. In this search, we find that it is not possible to obtain a good description of both the P_{11} and P_{33} phase shifts. The best joint fits to these two channels are shown as the dashed curves in Fig. 4. The resulting parameters are shown in the first row of

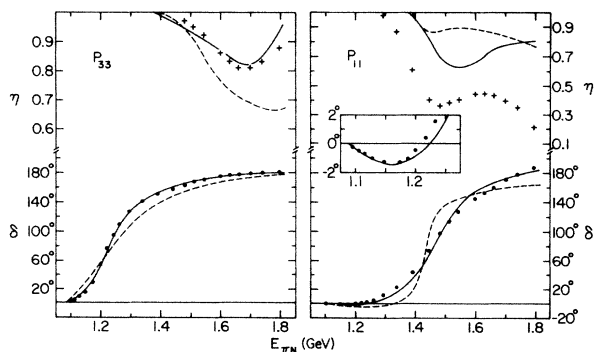


FIG. 4. Results of the fit to the P_{33} and P_{11} phase shifts. The dashed curves are the best joint fit to P_{11} and P_{33} neglecting $\pi\pi$ contributions. The solid curves show the improvement obtained by including diagrams like Fig. 1(c). The data are representative points from Refs. 2 and 3.

TABLE II. Bag model parameters giving the best fit to the πN P_{11} and P_{33} phase shifts. The first row neglects the $\pi\pi$ interactions and the second row includes the $\pi\pi$ terms.

	R (fm)	$f_{NN\pi}$	M_{Δ}^0 (MeV)	$M_{N^*}^0$ (MeV)
$V_{\pi\pi}=0$	0.850	1.125	1551	1704
$V_{\pi\pi}\neq 0$	0.865	1.080	1558	1737

Table II. The main difficulty in this fit is to reproduce the energy dependence of the P_{11} phase. The sign change in this channel is due to the cancellation between the repulsive nucleon pole term and the attraction coming from the N^* pole and all crossed terms [Fig. 1(b)]. The magnitudes of these two cancelling terms are mainly determined by the bag radius R . As R is decreased, both terms are increased at about the same rate and hence the sharp, rising energy dependence at $E \sim 1.3$ GeV cannot be removed for any value of R . This result is similar to that reported by Rinat.¹³ Another important finding in our search is that a large part of the attraction comes from the crossed terms. As shown in Fig. 5, when the crossed terms are also set to zero, the P_{11} phase shifts become more repulsive at low energy and the energy dependence is steeper in the sign-change region.

Without including the $\pi\pi$ scattering term, the fit to the P_{33} channel (dashed curves in Fig. 4) is also unsatisfactory. The dependence of δ on energy is not correct and the resulting inelasticity η is too large. Note that the fit to the low energy P_{33} phase shift can be easily obtained in a fit without considering the inelasticity and the related P_{11} phase shift. But as we stressed before, at the 2π level the P_{11} and P_{33} are determined by the same set of parameters. Such a low energy one-channel fit cannot be used to relate the πN data to the underlying pion-quark physics.

The results of including the $\pi\pi$ scattering term $V_{\pi\pi}$ [Fig. 1(c)] are shown as the solid curves in Fig. 4. The effect of $V_{\pi\pi}$ not only allows the model to give an excellent

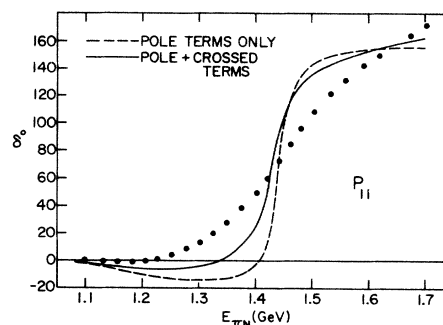


FIG. 5. Contributions to the P_{11} amplitude from the driving terms of Figs. 1(a) and (b). The dashed curve shows the phase shifts resulting from only the N and N^* pole terms. The solid curve is obtained by adding the crossed terms with N , Δ , and N^* intermediate states.

reproduction of the P_{33} phase shift in the entire energy region up to 2 GeV, but it also yields a correct description of the delicate sign change in the P_{11} channel. This dramatic improvement is probably due to the fact that the $\pi\pi$ scattering term $V_{\pi\pi}$ in the P_{11} channel is attractive and depends only weakly on the collision energy in the low energy region. This background attraction is needed to smooth away the sharp energy variation due to the cancellation involved in the pole and the crossed terms. The fit to this important P_{11} property is not accidental since the same $V_{\pi\pi}$ also plays a key role in obtaining an excellent fit in the P_{33} channel. While the inelasticity in P_{33} is well reproduced, there is still not enough inelasticity in P_{11} . This is not surprising since the P_{11} at high energy is also influenced by other open channels, such as the η particle production which is beyond the present cloudy-bag model description.

The best fit parameters are shown in the second row of Table II. It is seen that the bag radius and πNN coupling constant obtained are not very different from the values determined in Ref. 12. Hence, we expect that the corresponding 2π effects on the static properties of the nucleon

are small, following the arguments given by Thomas.¹¹ On this ground, we believe that our model is not a pure phenomenological construction such as the models developed in Refs. 4–10. It makes contact with the essential features of the quark-pion physics.

In conclusion, we have shown that the effect due to pion scattering from the virtual pion cloud of a nucleon plays an important role in describing the πN scattering. It is an essential component in a dynamical interpretation of the P_{11} phase shift which involves a delicate sign change in the low energy region. Since the present model makes contact with the pion-quark dynamics, its off-shell behavior is much more realistic than in the existing separable πN models.^{4–6} It will be interesting to explore in the future how our model can be used in a unitary πNN calculation of NN and πd reactions, such as that formulated in Refs. 4, 5, and 17.

This work was supported by the U.S. Department of Energy, Nuclear Physics Division, under Contract W-31-109-ENG-38.

¹See for example, M. Betz and T.-S. H. Lee, Phys. Rev. C 23, 375 (1981).

²G. Rowe, M. Salomon, and R. H. Landau, Phys. Rev. C 18, 584 (1978).

³D. J. Herndon *et al.*, CERN Theoretical Phases, UCRL Report No. UCRL-20030 (1970).

⁴T. Mizutani and D. S. Koltun, Ann. Phys. (N.Y.) C10, 109 (1977).

⁵For example, B. Blankleider and I. Afnan, Phys. Rev. C 31, 1380 (1985).

⁶B. Blankleider and G. E. Walker, Phys. Lett. 152B, 297 (1985).

⁷R. J. McLeod and I. R. Afnan, Phys. Rev. C 32, 222 (1985).

⁸R. L. Crawford *et al.*, Rev. Mod. Phys. 52, S25 (1984).

⁹T.-S. H. Lee, Phys. Rev. C 29, 195 (1984).

¹⁰R. S. Bhalerao and C. L. Liu, Phys. Rev. Lett. 54, 865 (1985).

¹¹A. W. Thomas, in *Advances in Nuclear Physics*, edited by J. W. Negele and Erich Vogt (Plenum, New York, 1983), Vol. 13, pp. 1–137.

¹²S. Theberge, A. W. Thomas, and G. W. Miller, Phys. Rev. D 22, 2838 (1980).

¹³A. S. Rinat, Nucl. Phys. A377, 341 (1982).

¹⁴G. E. Brown, J. W. Durso, and M. B. Johnson, Nucl. Phys. A397, 447 (1983).

¹⁵S. Theberge and A. W. Thomas, Nucl. Phys. A393, 252 (1983).

¹⁶B. R. Martin, D. Morgan, and G. Shaw, in *Pion-Pion Interactions in Particle Physics* (Academic, London, 1976), pp. 87–101, and references therein.

¹⁷T.-S. H. Lee and A. Matsuyama, Phys. Rev. C 32, 516 (1985).